Microchemical Journal 208 (2025) 112256

Contents lists available at ScienceDirect

Microchemical Journal

journal homepage: www.elsevier.com/locate/microc

Evaluation of CRISPR-Cas9 mismatch activity using a BRET-based reporter system

Tobias Wimmer [a,*], Anthony Lorenz [a], Lars Thomas Hossfeld [a], Surya Prakash Goud Ponnam [b], Lyubomyr Lytvynchuk [a], Knut Stieger [a]

[a] Department of Ophthalmology, Justus-Liebig-University Giessen, Germany
[b] Department of Molecular Biology and Biotechnology, School of Sciences, Tezpur University, PO: NAPAM, District: SONITPUR, Assam PIN: 784028, India

ARTICLE INFO

Keywords:
Bioluminescence Resonance Energy Transfer (BRET) Reporter System
Cellular reporter assay
CRISPR-Cas
sgRNA/DNA mismatch

ABSTRACT

CRISPR-Cas has revolutionized molecular biology, offering unparalleled precision and versatility in genome editing. CRISPR-Cas, originally part of the bacterial immune system, allows for the targeted modification of specific DNA sequences within living organisms. Of the many CRISPR-Cas systems, Cas9 has been used most frequently and applications have reached clinical stage in rare diseases. The system uses single guide RNA molecules to direct the Cas9 enzyme to specific DNA sequences, where it induces double-strand breaks. However, CRISPR-Cas9 can tolerate single-base mismatches between the sgRNA and the target DNA, potentially leading to off-target effects and challenges in achieving precision in high fidelity editing. With the evaluation of mismatch repair activity of wild-type CRISPR-Cas9 using a bioluminescence resonance energy transfer (BRET) based reporter system and by leveraging the BRET's sensitivity, we aim to quantify and characterize the cleavage events in mismatched sgRNA-Cas9/DNA interactions to predict off-target activity of a given sgRNA. This will improve the accuracy and reliability of CRISPR-Cas9 based genome editing. The robust reporter platform will enhance the refinement of CRISPR-Cas9 variants and facilitate the rational design of sgRNAs, ultimately improving the safety and efficacy of CRISPR-based therapeutic applications.

1. Introduction

The advent of the CRISPR-Cas (Clustered Regularly Interspaced Short Palindromic Repeats- CRISPR-associated protein) system has marked a paradigm shift in the field of molecular biology, offering unprecedented precision and versatility in genome editing. It constitutes a powerful RNA-guided gene-editing platform that allows the targeted modification of specific DNA sequences within the genome of living organisms. Originally discovered as part of the bacterial immune system with many different classes spread all over the bacterial kingdom, CRISPR-Cas9 has been the first and most frequently used system adapted for genome editing purposes, enabling scientists to selectively add, delete, or alter genetic material with remarkable efficiency [1]. The system's simplicity, cost-effectiveness, and applicability across diverse species have rapidly propelled it to the forefront of genetic engineering methodologies [2].

The CRISPR-Cas9 system utilizes single guide RNA (sgRNA) molecules to direct Cas9 to specific DNA sequences, where it induces DNA double-strand breaks (DSBs). The cell's natural repair mechanisms then come into play, allowing DSB repair [3]. Among all DSB repair mechanisms Non-Homologous End Joining (NHEJ) and Microhomology-Mediated End Joining (MMEJ) are responsible for off-target mutagenic effects. NHEJ can introduce insertions and deletions (indels) at the repair site, due to its mutagenic nature, which can have significant biological implications like on- and off-target effects. MMEJ, which is also inherently error-prone, often leads to larger deletions due to the end resection process searching for micro-homologous sequences. HR, in contrast is an error-free repair mechanism that is active primarily in the S and G2 phases of the cell cycle does not account for off-target effects [4]. Advancements such as the development of base editing and prime editing techniques have further enhanced the system's capabilities, allowing for more nuanced modifications, including point mutations and gene insertions that have a dramatically reduced mutagenic indel formation rate caused due to improper DSB repair [5,6].

The canonical CRISPR-Cas9 mechanism involves the formation of a sgRNA-DNA hybrid, guiding the Cas9 nuclease to its target sequence for

* Corresponding author at: Department of Ophthalmology, Justus-Liebig-University Giessen, Aulweg 123, 35392 Giessen, Germany.
E-mail address: tobias.wimmer@augen.med.uni-giessen.de (T. Wimmer).

https://doi.org/10.1016/j.microc.2024.112256
Received 7 November 2024; Received in revised form 19 November 2024; Accepted 21 November 2024
Available online 30 November 2024

cleavage. However, researchers have demonstrated that CRISPR-Cas9 can tolerate single-base mismatches between the sgRNA and the target DNA [7]. This mismatch tolerance can lead to unintended off-target effects thereby raising concerns about the specificity of the system. The ability of CRISPR-Cas9 to recognize and cleave DNA sequences with partial homology poses challenges in achieving absolute precision in genome editing. Understanding the factors influencing mismatch recognition is crucial for minimizing off-target effects and enhancing the reliability of CRISPR-Cas9-mediated genome editing [8]. Several factors contribute to the mismatch tolerance of CRISPR-Cas9, including the length and structure of the sgRNA, as well as the sequence context surrounding the target site [9]. The use of truncated or modified sgRNAs together with Cas9 can overcome unwanted off-target cleavage due to the decreased mismatch tolerance [10]. Ongoing research aims to elucidate the intricacies of these factors and develop strategies to mitigate the off-target effects, which enhances the fidelity of the CRISPR-Cas9 system including the engineering of Cas9 variants with reduced mismatch tolerance. Rational design approaches have focused on modifying the protein's structure to improve sgRNA binding specificity and decrease off-target effects. Researchers have developed high fidelity Cas9 variants, such as eSpCas9 and HypaCas9 that exhibit reduced off-target activities compared to their wild-type counterparts [11–13]. Additionally, advanced computational algorithms and bioinformatics tools have aided in the design of sgRNAs with minimal potential for mismatches [14].

To assess the fidelity of CRISPR-Cas9 systems, sophisticated methods were employed for genome-wide profiling of off-target effects [15,16]. While CRISPR RGEN Tools utilize algorithms to predict off-target sites based on sequence homology, tools like CRISPOR and CHOPCHOP offer comprehensive databases and scoring systems [17–19]. *In-vitro* methods, such as CIRCLE-Seq involve sgRNA-Cas9 digestion and sequencing of genomic DNA to identify off-target sites with high sensitivity and accuracy [20,21]. *In-vivo* methods like GUIDE-Seq integrate oligonucleotides at Cas9-induced breaks in living cells, followed by sequencing to map off-target activity, while SITE-Seq combines *in-vitro* digestion with high-throughput sequencing for potential off-target site identification [15,22]. High-throughput screening methods like HTGTS (High-Throughput Genome-wide Translocation Sequencing) detect the CRISPR-Cas9-induced chromosomal translocations, offering insights into genome-wide off-target effects [23]. These techniques allow researchers to identify and characterize the potential off-target sites, facilitating the validation of system improvements and the continuous refinement of high fidelity platforms.

Bioluminescence resonance energy transfer (BRET)-based reporter systems have emerged as powerful tools in biological research, offering real-time, non-invasive monitoring of cellular and molecular processes. These systems leverage the non-radiative energy transfer between a bioluminescent donor and a suitable fluorescent acceptor, allowing for specific detection of molecular interactions and changes *in-vitro* and *in-vivo* [24–26]. BRET is a highly sensitive tool for monitoring molecular interactions, particularly in dynamic biological processes like protein–protein interactions or receptor dimerization. Its sensitivity to proximity makes it ideal for studying subtle molecular changes such as the binding of compounds like maltose or vascular endothelial growth factor (VEGF) [24,27–30]. BRET relies on the energy transfer between a bioluminescent donor and a fluorescent acceptor, using the emission of light from the donor protein, such as *Renilla Reniformis* luciferase, converting its substrate coelenterazine, which minimizes interference and preserves the integrity of live cells during imaging due to its low toxicity at commonly applied doses [31]. The combination of BRET with CRISPR/Cas for diagnosis was established during the SARS-CoV 2 pandemic using the so called dead (inactive) but still target binding Cas9 variants. Binding to viral SARS-CoV 2 DNA in sample material was detected via BRET analysis measured with a simple camera device [32].

In the context of Cas9 genome editing, BRET is still an expanding niche but has the potential to be established as a powerful tool for studying DNA repair dynamics. For example, it has been employed to track Homology-Directed Repair with an acceptor HDR template after DSB induction mediated by a luciferase tagged Cas9 endonuclease in both CXCR4 and ß-arrestin 2 loci [33]. The basis of this study described the assessment of the activity of sgRNA-Cas9 complexes using the mutagenic effect of NHEJ on shifting the reading frame due to indel formation in combination with DNA repair pathway engineering, inhibiting essential repair proteins [34]. A big advantage of BRET based reporter systems is it is non-invasive character, wherein there is no need for external light excitation. This feature significantly reduces the risk of phototoxic effects, that can occur when cells are exposed to high-intensity light during fluorescence imaging. Phototoxicity can lead to cellular damage or affect cellular behavior, thus compromising experimental results [35].

The aim of this study is to evaluate the mismatch activity of CRISPR-Cas9/sgRNA complexes using a BRET-based reporter system. By leveraging the sensitivity of BRET, we intend to precisely quantify and characterize cleavage events of the mismatched sgRNA-Cas9/DNA hybrids. By implementing BRET reporter's specificity to potential off-target sites and assessing their activity in a cellular assay, we aim to enhance the accuracy and reliability of CRISPR-Cas9 genome editing. This robust platform for detecting unintended genomic alterations would improve the refinement and optimization of CRISPR-Cas9 variants and facilitate the rational design of sgRNAs.

2. Material and methods

2.1. BRET reporter plasmids

BRET reporter plasmids were derived from previously described plasmids [34]. A shuttle cloning box containing *AvrII* and *BsiWI* restriction sites was introduced between the reading frames of the BRET donor RLuc8 and the BRET acceptor GFP2, allowing the in-frame insertion of the CRISPR/Cas9 mismatch target sequences containing the Protospacer Adjacent Motif (PAM) together with a surrounding sequence context. For the introduction of Cas9 target sequences into the BRET reporter, restriction digestion with *AvrII* and *BsiWI* (NEB, Frankfurt, Germany) was carried out overnight at 37 °C. Double-stranded target sequences were generated by the hybridization (98 °C, 10 min. followed by 20 °C, 30 min.) of wild-type/mismatch oligonucleotides (Metabion, Planegg, Germany) with 4 bp overhangs complementary to the *AvrII/BsiWI*-digested BRET reporter. After ligation and transformation into E. coli XL1 (Stratagene/Qiagen, Hilden, Germany), individual clones were further analyzed for the correct integration and orientation by Sanger sequencing, propagated, and the plasmid DNA was isolated and purified for mammalian transfection using commercial kit.

2.2. Cloning and purification of sgRNA-Cas9 plasmid for mammalian transfection

sgRNA-Cas9 plasmid pSpCas9(BB)-2A-Puro (px459) (addgene: #62988) was used as Cas9 expressing and sgRNA transcribing plasmid [36]. Plasmid was digested with *BbsI* (NEB, Frankfurt, Germany) overnight at 37 °C. Complementary oligonucleotides coding for the sgRNA sequenced containing 4 bp overhangs for *BbsI* cloning were hybridized (98 °C; 10 min. followed by 20 °C; 30 min.) to form a double stranded DNA molecule for the ligation with the previously hydrolyzed px459. After transformation into E. coli XL1, individual clones were analyzed by sequencing; positive clones were also propagated and the plasmid DNA was isolated and purified for mammalian transfection using commercial kit (Qiagen, Hilden, Germany).

2.3. Cell culture

HEK293-T (Human Embryonic Kidney; ATCC: CRL-3216) cells were cultured in DMEM (Dulbecco's modified Eagle's medium) (Anprotec, Bruckberg, Germany) supplemented with L-Glutamine (4 mM; PAN Biotech, Aidenbach, Germany), Penicillin/Streptomycin (100 IU/mL; 0.1 mg/mL; Anprotec, Bruckberg, Germany), and 10 % FBS (Fetal Bovine Serum; PAN Biotech, Aidenbach, Germany). Incubation was carried out at 37 °C, 5 % CO_2, in a humidified incubator. At confluence, cells were detached using Accutase (Anprotec, Bruckberg, Germany), diluted (1:10) with supplemented DMEM, and transferred into fresh culture dishes (Greiner, Frickenhausen, Germany).

2.4. Polyethylenimine (PEI) transfection

One day prior to transfection, cells were detached as described earlier and seeded at a density of 200,000 cells/well in six-well plates (Greiner, Frickenhausen, Germany), and incubated for 24 h as mentioned earlier in the cell culture chapter. On the day of transfection, the culture media was replaced with 1.5 mL fresh supplemented DMEM. Plasmid DNA (2.0 μg BRET reporter plasmid ± 2.5 μg sgRNA-Cas9 plasmid) was diluted in 100 μL sterile 150 mM NaCl followed by the addition of 200 μl of 1.0 mg/mL PEI (MW: 40,000, Polysciences, Hirschberg, Germany). After 10 min of incubation at room temperature, the transfection mix was added dropwise to the cells in the six well plate. To avoid cellular stress, the culture media was replaced 4–6 h post transfection, after which the cells were incubated for additional 24 h.

2.5. Cell lysis

For cell lysis, the culture media from the transfected cells was removed, and cells were washed once with sterile 1x PBS (Phosphate-Buffered Saline). Renilla luciferase assay lysis buffer (100 μL/well; Promega, Mannheim, Germany) was added, cells were collected with a cell scraper and resultant cell suspension was transferred into a new tube for cell lysis in liquid nitrogen with two freeze–thaw cycles. The debris from the samples were cleared by following centrifugation at 17,986 x g at 4 °C for 10 min. and then transferring the clear solution into a new tube for storage at −20 °C or until further use.

2.6. BRET reporter assay

5.0 μl of the clarified cell extract was plated per well in 96-well plates (COSTAR Lumiplates FlatWhite; Corning, NY, USA). Rluc8 substrate stock (Coelenterazine 400a, Nanolight Inc., Pinetop AZ) (1.0 mg/mL), was diluted 1:100 in 1x PBS (final conc: 10.0 μg/mL) and allowed to stabilize under light protection for 20 min. The diluted substrate (100 μl/well) was injected automatically and readings were taken immediately after substrate injection using the BRET transmission filter set (blue filter: 370–450 nm; green filter: 510–540 nm) of the plate reader (Tecan Infinite M1000Pro, Tecan, Groeding, Austria) with an integration time of 1 s.

2.7. Fluorescence Microscopy

Qualitative GFP2 expression of the BRET reporter was shown using the Keyence BZ-8000 (Keyence, Neu-Isenburg, Germany) with a maximal exposure time of 0.5 s.

2.8. Statistics and calculations

2.8.1. Statistics

Unless otherwise stated, each experiment was conducted in triplicate, with quadruple measurements in the BRET assay. For statistical analysis, the Mean ± SD (Standard Deviation) of the triplicates were used. To achieve normal distribution, the data were logarithmically transformed. The normal distribution was verified using the Shapiro-Wilk test. To determine p-values for comparisons between two groups, the unpaired Student's *t*-test was used when data were normally distributed. For comparisons among multiple groups, ANOVA was used if data was normally distributed. P-values < 0.05 (*) were considered as statistically significant, p-values < 0.01 (**) as highly statistically significant and p-values < 0.001 (***) as statistically very high significant. Means ± SD resulting from the BRET assay were used to calculate the frameshift rate [%]. The frameshift rate was always defined as ≥ 0 %. Negative values are caused by measurement fluctuations and were marked as not detectable (nd).

2.8.2. Calculations

BRET Ratio:

The BRET Ratio [BU] (BRET Units) of each sample was calculated by dividing the GFP2 (photons/second) by the RLuc8 (photons/second [p/s]) output.

$$BRETRatio[BR] = \frac{Int.GFP2\left[\frac{p}{s}\right]}{Int.RLuc8\left[\frac{p}{s}\right]}$$

Frameshift-Rate:

The conversion of the BRET Ratios [BU] to the Frameshift Rate [%] was calculated according the following equation [34]

$$FrameshiftRate[\%] = \left(1 - \frac{(MeanBR \pm SD(Target + sgRNA - Cas9) - MeanBR \pm SD(RLuc8)}{(MeanBR \pm SD(Target) - MeanBR \pm SD(RLuc8)}\right) x100$$

3. Results

Understanding mismatch tolerance and implementing methods to assess off-target activity is crucial for enhancing the specificity and safety of CRISPR-based therapeutic approaches. Quantifying the activity of mismatched sgRNA-Cas9/DNA complexes can provide useful information about the position and nucleotide-specific activity to introduce unwanted mutations within the genome.

3.1. BRET reporter sensitively measures mismatch cleavage effects

The BRET reporter used to assess the cleavage activity of partially mismatched sgRNA-Cas9/DNA hybrids relies on the disruption of the reading frame of the BRET acceptor fluorophore GFP2 caused by the insertion and deletion of nucleotides after a DSB through NHEJ and/or MMEJ, while the BRET donor RLuc8 remains unaffected (Fig. 1A). Compared to the non-mismatched WT target and sgRNA-Cas9 binding, mismatched binding shows higher BRET ratios, leading to lower frameshift rates. Due to the simple and rapid cloning procedure using the shuttle box present in the BRET reporter construct, we were able to test all 60 possible nucleotide substitutions over the 20 bp of the target DNA sequence hybridized to sgRNA-Cas9 (Fig. 2; Supplement Table 1 for mismatched DNA target sequences). Compared to the wild-type (WT) control, which shows the highest reduction of the BRET ratio, mismatch cleavage activity clustered depending on their position. Mismatches at the PAM-distal and PAM-proximal regions (positions 18–20 and 1–12)

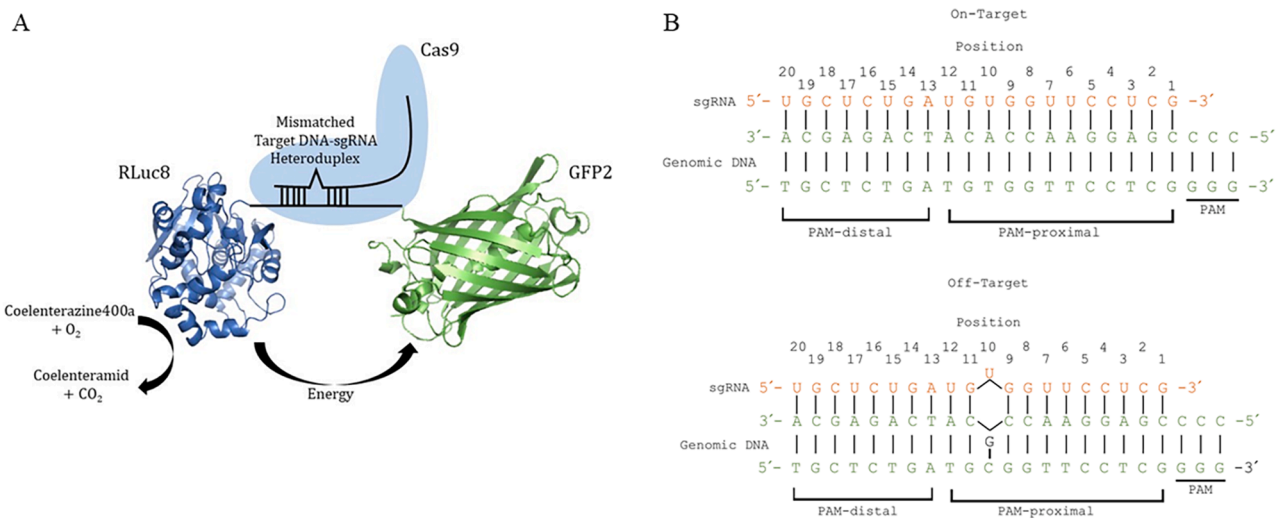

Fig. 1. BRET-Based CRISPR/Cas9 Mismatch Activity Quantification Principle. (A) Residual sgRNA-Cas9 activity on a mismatched target sequence is measured by the BRET reporter system. The sgRNA-Cas9 complex binds to the target sequence and generates a mismatched sgRNA-DNA heteroduplex located between the BRET reporters' reading frames of the energy donor RLuc8 and the energy acceptor GFP2. This induces a DSB at the targeted site upon mismatch activity. Subsequent NHEJ repair generates indels at the DSB site, shifting the reading frame of the acceptor, which reduces the ratio of I_{GFP2}/I_{RLuc8}. (B) Examples of On-Target and Off-Target cleavage: On-Target: Perfect binding of sgRNA to genomic DNA, resulting in optimal sgRNA-Cas9 mediated cleavage. Off-Target: Imperfect binding to genomic DNA with a mismatch at e.g. position 10 leads to reduced cleavage activity compared to a perfect match.

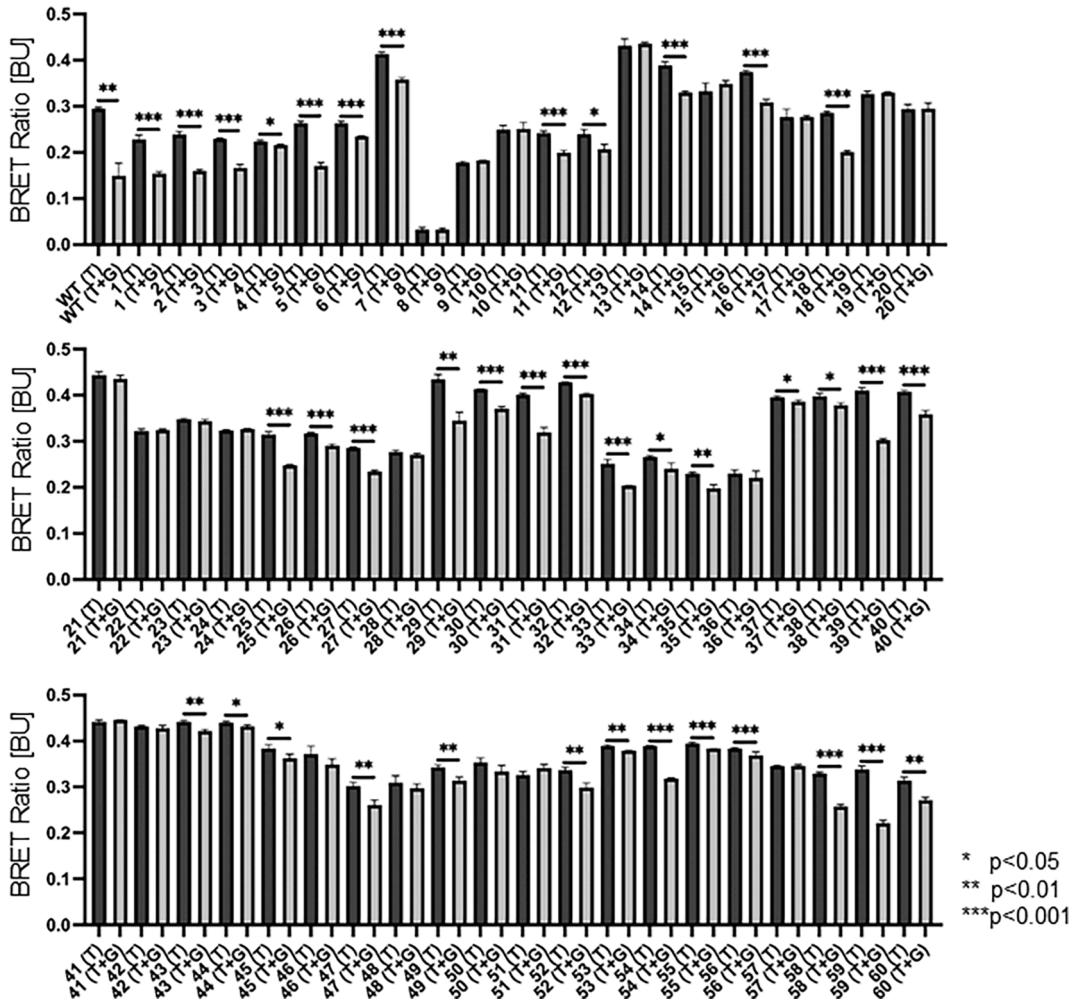

Fig. 2. BRET Measurements. BRET ratios of a perfectly matched sgRNA/DNA duplex (WT (Target [T])/WT (Target + sgRNA-Cas9 [T + G])) compared to all three possible combinations of mismatches at each position of the 20 bp target sequence. (*p < 0.05; **p < 0.01; ***p < 0.001).

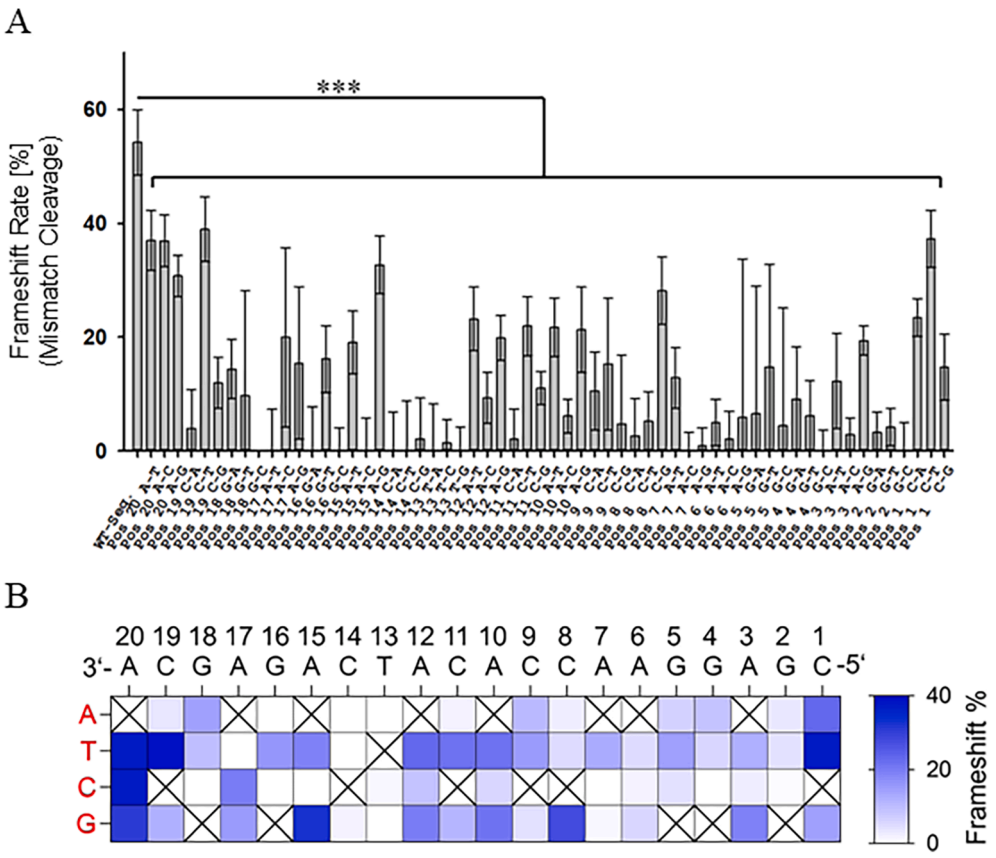

Fig. 3. Mismatch frameshift rate. (A) Conversion of the BRET ratio to the frameshift rate [%] for all possible mismatch combinations at each position of the target site. (***$p < 0.001$) (B) Heat map visualization of mismatch cleavage activity of a given sgRNA-Cas9 complex on a mismatched target sequence in dependence of the target sequence position.

allowed mismatch cleavage, which led to frameshifting mutations, as measured by a reduction in the BRET ratio. At positions 13–17, mismatched hybrids showed no or only a slight reduction in the BRET ratio, suggesting low mismatch cleavage activity.

The transformation from BRET ratio to the frameshift rate corroborated the initial results, clearly showing the reduction of mismatch activity between positions 13–17 (Fig. 3A). The frameshift rate heat map shows a high acceptance of mismatches in the PAM distal and PAM proximal parts, although at positions 1–7, mismatch cleavage is reduced compared to positions 19–20. Notably, a conversion to cytosine (C) at position 1–7 outperformed all other substitutions in terms of reduced mismatch cleavage activity (Fig. 3B). To further verify the quantified results from the BRET reporter assay, we qualitatively observed a reduction in GFP2-positive cells and GFP2 intensity in transfected HEK293-T cells compared to the negative control (BRET reporter/–sgRNA-Cas9) (Fig. 4). Consistent with the BRET data, at the far distal position 20 of the hybrid, almost no GFP2 positive cells with low fluorescence intensities could be detected by fluorescence microscopy while at position 14, little to no reduction in GFP2 expression was observed. In line with this, at the closest distal position to PAM (position 1), a reduced amount and intensity of GFP2 fluorescence was detected, indicating mismatch cleavage.

3.2. *Mismatch cleavage is position and nucleotide substitution dependent*

After evaluating and verifying the acceptance of mismatch cleavage, we delved deeper to understand how single nucleotide substitutions affect mismatch cleavage with subsequent DNA repair (Fig. 5). Conversions from the wild-type sequence to adenine (A) generally showed low (< 20 %) acceptance of mismatch cleavage across all positions tested, with one exception at position 1, where we measured the highest acceptance of an A, leading to a frameshift rate of > 20 % (Fig. 5A). Conversions to thymidine (T) from the wild-type sequence presented a different scenario. Mismatches at positions 19–20 and 1 were highly accepted, whereas positions 14 and 17 showed only minor acceptance. All other positions exhibited reduced mismatch activity, ranging from 10-30 % (Fig. 5A). Conversions from the wild-type sequence to cytidine (C) revealed another pattern. Mismatch cleavage was allowed at the far PAM distal part at positions 17–20, but greatly reduced at all remaining PAM proximal and distal positions of the sgRNA-Cas9/DNA hybrids. Conversions from the wild-type sequence to guanine (G) showed moderate mismatch cleavage activity across the whole sgRNA-Cas9/DNA hybrid, except at positions 7 and 13–14, where no mismatch cleavage activity was observed (Fig. 5A).

Subsequently, we grouped the mismatch cleavage activity to the four nucleotides to eliminate the position dependence. Interestingly, we found that thymidine as a pyrimidine base and guanine as a purine base with a mean mismatch activity ranging from 14-16 % frameshift rate outperformed adenine- (purine) and cytosine-bases (pyrimidine) in mismatch cleavage activity, which showed a lower mean activity between 4–6 % (Fig. 5B). To show position dependence, we took our data on mismatch cleavage and eliminated the nucleotide context. The far PAM distal and the near PAM proximal region showed the highest acceptance for mismatch cleavage, ranging between approx. 30–40 % frameshift rate. Between these regions, mismatch cleavage activity is reduced to around 20 %. We also could demonstrate with this experiment that mismatched nucleotides at position 6–8 and 14 do not allow cleavage irrespective of the nucleotide that is being substituted (Fig. 5C).

Further, we separated our data individually for purine (Pur) and

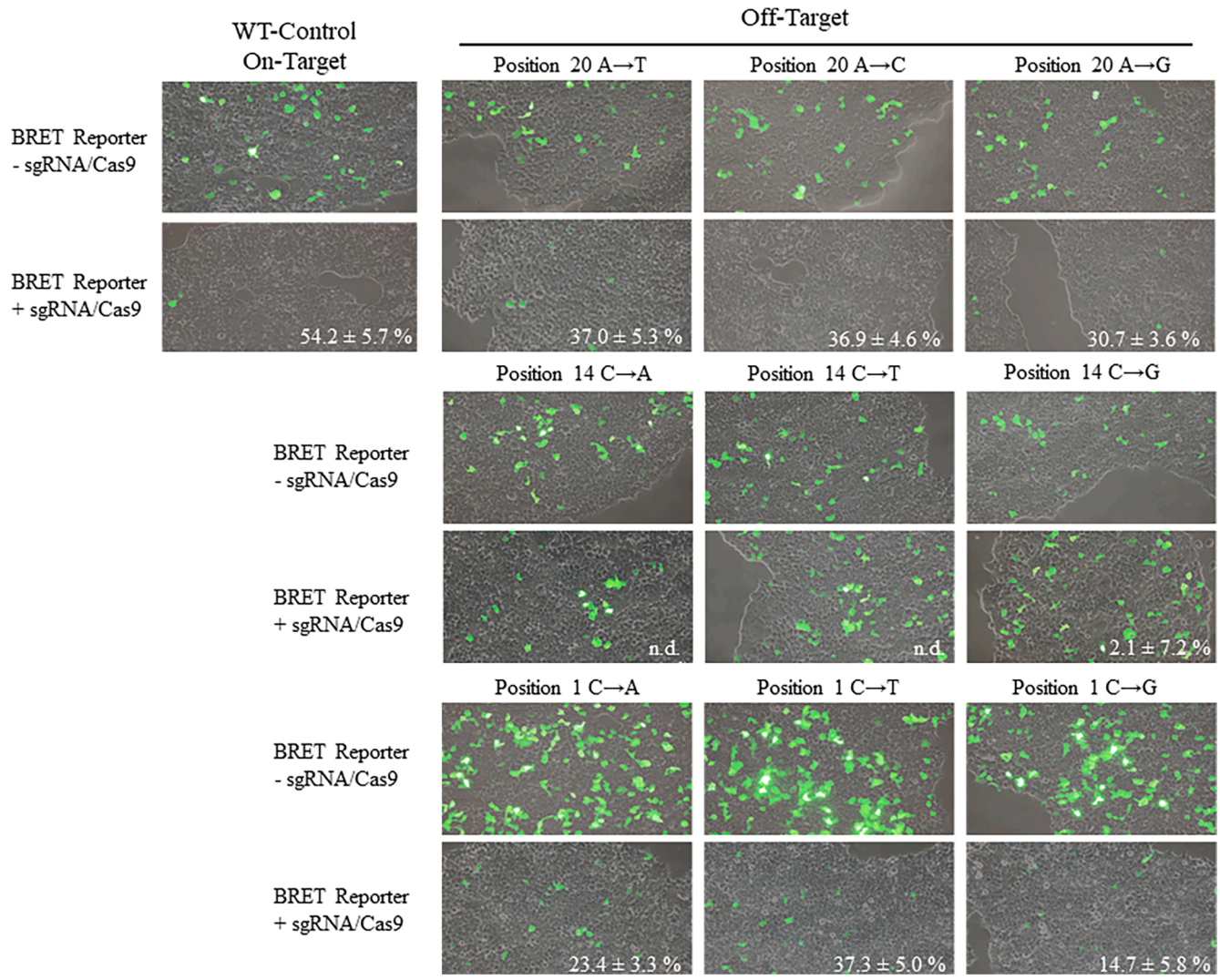

Fig. 4. Qualitative mutagenic frameshift analysis. Fluorescence microscopy of the reduced GFP2 expression of the BRET reporter caused by mutagenic, frameshifting indel formation upon mismatch sgRNA-Cas9 cleavage, compared to the WT-control.

pyrimidine (Pyr) base pairings to possibly find a dependence on the influence of different hydrogen bonding between these two groups of mismatched nucleotides (Fig. 6). We grouped the mismatch cleavage activity for Pyr-Pyr, Pur-Pur, Pyr-Pur, and Pur-Pyr nucleotides at different positions of the sgRNA-Cas9/DNA hybrid (Fig. 6 A). The Pyr-Pyr (T-U) mismatch pairing showed the typical position-dependent cleavage activity already seen in previous experiments, at the far distal region (position 20) with a significant drop with almost no mismatch cleavage at position 17. On contrary, Pyr-Pyr (C-C) mismatches showed almost no or just low cleavage activity over all positions tested. Between positions 3–15, moderate mismatch cleavage was observed again. Pur-Pur (G-G) mismatches, in contrast, showed moderated cleavage activity in the PAM distal region, while cleavage was increased at distal positions. Pyr-Pur (C-T) mismatches clearly showed, as the already described Pyr-Pyr combination T-U, the typical mismatch cleavage pattern where the far distal position 20 allowed high frequencies of up to ≈ 40 %, followed by a massive drop between positions 6–15 and a slight increase in mismatch cleavage in the proximal region. For both Pur-Pyr combinations, A-G and A-C generally exhibited the lowest mismatch cleavage activity over all positions tested, except for the nearest proximal position 1 for the A-G mismatch sgRNA-Cas9/DNA hybrid. To further condense the position-specific data to a more general bias, we grouped the data as described before using Pyrimidine and Purine groups. Both Pyr-Pyr and Pur-Pur combinations with relatively high mismatch cleavage activity, ranging from 18-22 %, outperformed Pyr-Pur and Pur-Pyr with a maximum of allowed mismatch cleavage of approximately 10 % (Fig. 6B).

To finalize our reporting, we performed two additional experiments to prove the system's reliability with an enhanced version of SpCas9 with a reportedly decreased mismatch cleavage activity and the sensitivity with allowance for cleavage with different double mismatches on-target DNA (Supp.Fig. 1). First, we compared our WT SpCas9 with an (enhanced) eSpCas9(1.1) version in the BRET assay followed by the transformation into the frameshift rate (Supp.Fig. 1A). We found a highly significant (***$p < 0.001$) increase in the BRET ratio when using the enhanced Cas9 variant, and subsequent data transformation confirmed these findings with a high significant reduction (**$p < 0.01$) in the frameshift rate. Double sgRNA-Cas9/DNA mismatched hybrids, compared to single mismatches, showed a highly significant (***$p < 0.001$) reduction of mismatch tolerance over all positions and combinations tested, not exceeding 10 % of mismatch cleavage activity (Supp. Fig. 1B).

4. Discussion

BRET based reporter assays are extremely sensitive even though they require relatively simple assay setups compared to other assays including fluorescent methods [37]. A low background noise makes

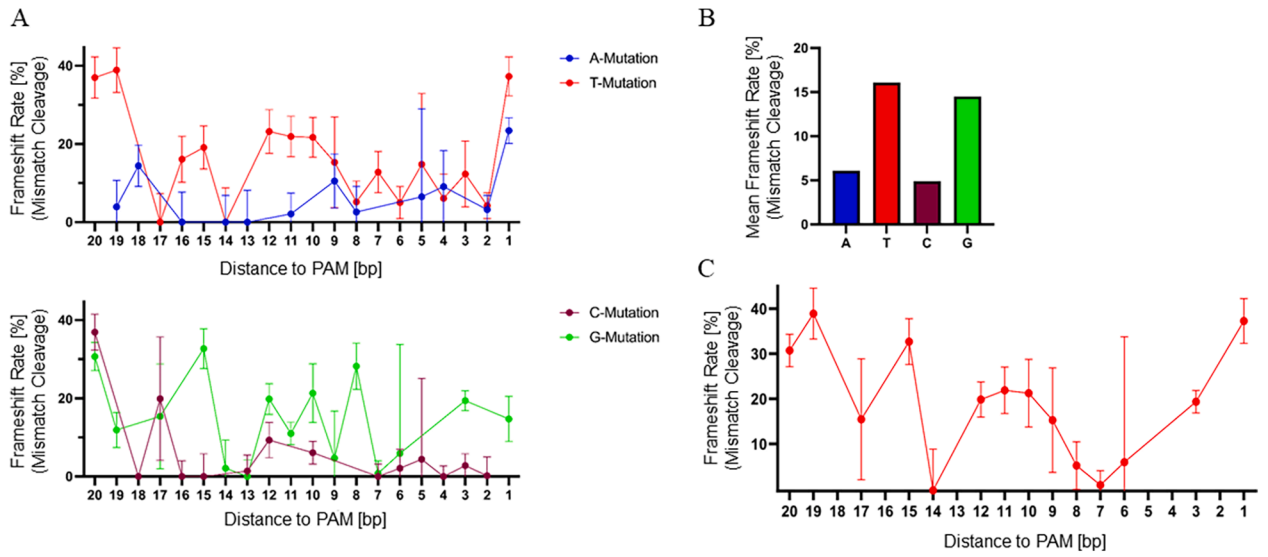

Fig. 5. Target sequence position dependent mutations and their influence on sgRNA-CAs9 cleavage activity. (A) Influence of WT to Adenine mutations (blue), WT to Thymidine mutations (red), WT to Cytosine mutations (brown) and WT to Guanosine mutations (green) on position dependent mismatch sgRNA-Cas9 cleavage activity. (B) Mean of combined sgRNA-Cas9 cleavage activity from WT sequence to an A, T, C and G. (C) Position dependent combined mismatch cleavage activity upon imperfect gRNA-DNA binding. (For interpretation of the references to colour in this figure legend, the reader is referred to the web version of this article.)

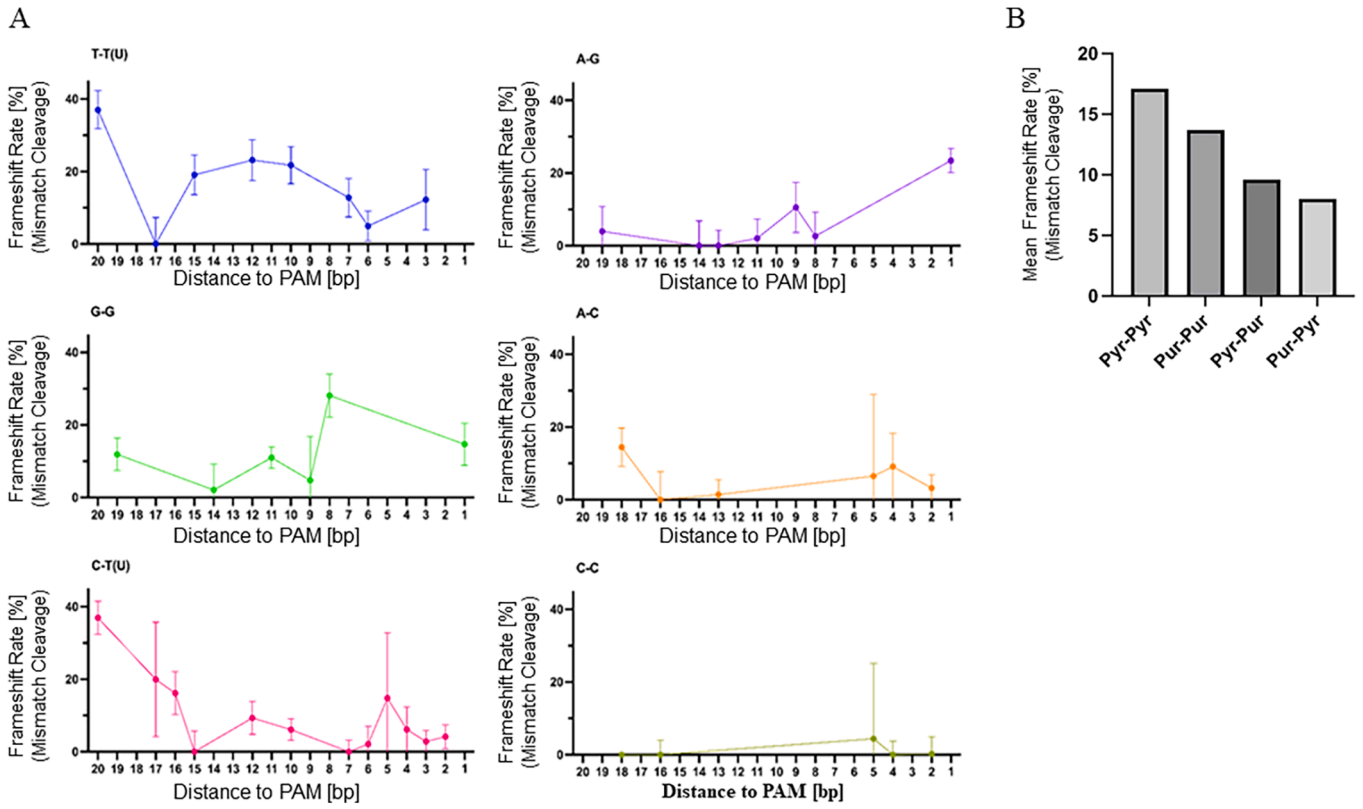

Fig. 6. CRISPR/Cas9 cleavage activity of homologous and heterologous purine and pyrimidine base exchange within the target sequence. (A) Frameshift rates [%] upon sgRNA-Cas9 mismatch cleavage in dependence of homologous and/or heterologous mismatching bases and position. (B).

these assays ideal for studying processes with low signal output as it is assumed for an accurate measurement of CRISPR-Cas9 mediated mismatch cleavage. Typically, they offer a broad dynamic range making them versatile for both qualitative and quantitative measurements. Especially the quantitative aspect together with the possibility for real-time *in-vivo* monitoring of processes in living organisms without the need to sacrifice the model organism for subsequent experiments makes BRET very interesting for researchers in genome editing [33]. Compared to other methods assessing off-target activity of mismatched DNA/sgRNA-Cas9 heteroduplexes, the BRET reporter system, even in combination with a preceded *in-silico* prediction, can give valuable information about mismatch cleavage activity on a selection of off-target sequences. Although this system is generally capable as a high-throughput system it only quantifies mismatched target sequences one

by one while more sophisticated, sequencing based methods like SITE-Seq or GUIDE-Seq deliver genome wide information with higher sensitivity and accuracy [15,38]. One of the major challenges in CRISPR-Cas9 mediated genome editing is the potential for off-target effects mediated by high mismatch cleavage activity of gRNAs on genomic DNA off-targets, which can lead to unintended modifications. Sophisticated methods like the BRET reporter system for the quantification of mismatch cleavage as described here in this study can help in understanding the factors responsible for mismatch recognition, which are crucial to minimize off-target effects and enhance the specificity of CRISPR-Cas9-mediated genome editing [39].

In this study, we were able to show that cleavage activity is clustered in defined areas upon their mismatch position within the sgRNA/DNA hybrid. Our data provide evidence that in the far distal region (position 20) mismatch cleavage is accepted at high frequencies. To overcome this effect, shorter, so-called truncated sgRNA (tru-sgRNA) have been described to decrease off-target cleavage activity. Interestingly on-target activity like the NHEJs indel formation and also HDR was influenced negatively [40]. Moreover, 5́-truncated sgRNA-Cas9 complexes have been shown to reduce mismatch tolerance by negative selection in bacterial genomes [10]. Another possible method to minimize off-target effects would be to chemically modify terminal and/or internal nucleotides of the sgRNA with 2′-O-methyl or phosphorothioate groups. It has been reported that these modifications reduce off-target effects while maintaining the original on-target activity. These sgRNA modifications can only be attached *in-vitro* to the previously transcribed sgRNA, with a subsequent complexing reaction with the Cas9 protein. This allows the use of alternative transfer methods like e.g. nanoparticle instead of adeno-associated virus (AAV) transduction [41]. Also, in the nearest PAM proximal position 1, mismatch cleavage is highly accepted depending on the mismatched nucleotide. This off-target activity already has been reported by several other groups, but depends on the general sgRNA sequence, the surrounding sequence and target PAM context [42–44]. PAM sliding from e.g. GGG to NGG resulted in an increased sgRNA-Cas9 specificity [43]. In general, we had observed a higher mismatch tolerances in the complete PAM proximal region from position 2–12. This cluster also covers the seed region which is usually the first 5 bp next to the PAM where a decrease of mismatch cleavage was reported in dependence of the sequence context [45].

Recent studies on the kinetics of sgRNA-Cas9 binding to off-target DNA sequences with a single molecule resolution focused on the structural changes of Cas9 in dependence of the position and type of nucleotide exchange compared to an on-target binding. For the binding of sgRNA-Cas9 to its target sequence a series of well-defined conformational rearrangement checkpoints takes place ensuring proper binding, moving catalytic domains to the correct position for cleavage or active pocket opening for DNA substrate binding. The target DNA itself acts as the determinant for these processes. Interestingly, mismatches had just a minor influence on these structural changes, enabling off-target cleavage activity [46]. Non-canonical purine and/or pyrimidine base pairings like wooble (G-U/T or A-C) or hoogsteen (A-G or G-G) nucleotide pairings due to the formation of hydrogen bonds can explain the relative high mismatch cleavage activity when separating the data to these nucleotide pairings [47]. High fidelity Cas9 variants, such as eSpCas9 or HypaCas9, that are protein engineered to improve the precision and specificity of CRISPR-Cas9 genome editing and exhibit reduced off-target activities compared to their wild-type counterparts. The development process involves several steps, including rational design, mutagenesis, and thorough validation. Typically, these residues interact with the DNA backbone or regions outside the PAM and guide RNA recognition site [48].

5. Conclusion

Various methods have been described that allow researchers to identify and characterize potential off-target sites, facilitating the validation of system improvements and the continuous refinement of high-fidelity platforms. Here, we provide an evidence that a BRET based sensor is sensitive enough to evaluate and quantify CRISPR-Cas9 off-target mismatch cleavage activity in a cellular context and with a single nucleotide resolution. Hence, a combination of *in-silico*, *in-vitro*, and *in-vivo* methods, along with improved Cas9 variants and sgRNA designs, can effectively assess and mitigate off-target effects. These advancements are crucial for the safe and accurate application of the CRISPR technology in research and in a therapeutic context.

CRediT authorship contribution statement

Tobias Wimmer: Writing – original draft, Supervision, Formal analysis, Conceptualization. **Anthony Lorenz:** Investigation, Formal analysis, Data curation. **Lars Thomas Hossfeld:** Investigation, Formal analysis, Data curation. **Surya Prakash Goud Ponnam:** Writing – review & editing, Methodology. **Lyubomyr Lytvynchuk:** Writing – review & editing, Methodology. **Knut Stieger:** Writing – original draft, Supervision, Methodology, Funding acquisition, Formal analysis, Conceptualization.

Declaration of competing interest

The authors declare the following financial interests/personal relationships which may be considered as potential competing interests: None of the authors has a financial interest to declare. T.W. and K.S. are holding a patent of the BRET reporter system.

Acknowledgements

This work was funded by the German Research Council DFG (DFG Sti 597/7).

Appendix A. Supplementary data

Supplementary data to this article can be found online at https://doi.org/10.1016/j.microc.2024.112256.

Data availability

Data will be made available on request.

References

[1] J.A. Doudna, E. Charpentier, Genome editing. The new frontier of genome engineering with CRISPR-Cas9, Science 346 (2014) 1258096, https://doi.org/10.1126/science.1258096.
[2] A.N. Ansori, Y. Antonius, R.J. Susilo, S. Hayaza, V.D. Kharisma, A.A. Parikesit, R. Zainul, V. Jakhmola, T. Saklani, M. Rebezov, M.E. Ullah, N. Maksimiuk, M. Derkho, P. Burkov, Application of CRISPR-Cas9 genome editing technology in various fields: A review, Narra J. 3 (2023) e184. https://doi.org/10.52225/narra.v3i2.184.
[3] A.C. Komor, A.H. Badran, D.R. Liu, CRISPR-Based Technologies for the Manipulation of Eukaryotic Genomes, Cell 169 (2017) 559, https://doi.org/10.1016/j.cell.2017.04.005.
[4] M. de Falco, M. de Felice, Take a Break to Repair: A Dip in the World of Double-Strand Break Repair Mechanisms Pointing the Gaze on Archaea, Int. J. Mol. Sci. 22 (2021), https://doi.org/10.3390/ijms222413296.
[5] A.V. Anzalone, P.B. Randolph, J.R. Davis, A.A. Sousa, L.W. Koblan, J.M. Levy, P. J. Chen, C. Wilson, G.A. Newby, A. Raguram, D.R. Liu, Search-and-replace genome editing without double-strand breaks or donor DNA, Nature 576 (2019) 149–157, https://doi.org/10.1038/s41586-019-1711-4.
[6] Y.B. Kim, A.C. Komor, J.M. Levy, M.S. Packer, K.T. Zhao, D.R. Liu, Increasing the genome-targeting scope and precision of base editing with engineered Cas9-cytidine deaminase fusions, Nat. Biotechnol. 35 (2017) 371–376, https://doi.org/10.1038/nbt.3803.
[7] T. Zheng, Y. Hou, P. Zhang, Z. Zhang, Y. Xu, L. Zhang, L. Niu, Y. Yang, D. Liang, F. Yi, W. Peng, W. Feng, Y. Yang, J. Chen, Y.Y. Zhu, L.-H. Zhang, Q. Du, Profiling single-guide RNA specificity reveals a mismatch sensitive core sequence, Sci. Rep. 7 (2017) 40638, https://doi.org/10.1038/srep40638.

[8] S.Q. Tsai, J.K. Joung, Defining and improving the genome-wide specificities of CRISPR-Cas9 nucleases, Nat. Rev. Genet. 17 (2016) 300–312, https://doi.org/10.1038/nrg.2016.28.
[9] P. Schindele, F. Wolter, H. Puchta, CRISPR Guide RNA Design Guidelines for Efficient Genome Editing, Methods Mol. Biol. 2166 (2020) 331–342, https://doi.org/10.1007/978-1-0716-0712-1_19.
[10] H.J. Lee, H.J. Kim, S.J. Lee, Mismatch Intolerance of 5'-Truncated sgRNAs in CRISPR/Cas9 Enables Efficient Microbial Single-Base Genome Editing, Int. J. Mol. Sci. 22 (2021), https://doi.org/10.3390/ijms22126457.
[11] B.P. Kleinstiver, V. Pattanayak, M.S. Prew, S.Q. Tsai, N.T. Nguyen, Z. Zheng, J. K. Joung, High-fidelity CRISPR-Cas9 nucleases with no detectable genome-wide off-target effects, Nature 529 (2016) 490–495, https://doi.org/10.1038/nature16526.
[12] I.M. Slaymaker, L. Gao, B. Zetsche, D.A. Scott, W.X. Yan, F. Zhang, Rationally engineered Cas9 nucleases with improved specificity, Science 351 (2016) 84–88, https://doi.org/10.1126/science.aad5227.
[13] J.S. Chen, Y.S. Dagdas, B.P. Kleinstiver, M.M. Welch, A.A. Sousa, L.B. Harrington, S.H. Sternberg, J.K. Joung, A. Yildiz, J.A. Doudna, Enhanced proofreading governs CRISPR-Cas9 targeting accuracy, Nature 550 (2017) 407–410, https://doi.org/10.1038/nature24268.
[14] M. Naeem, O.S. Alkhnbashi, Current Bioinformatics Tools to Optimize CRISPR/Cas9 Experiments to Reduce Off-Target Effects, Int. J. Mol. Sci. 24 (2023), https://doi.org/10.3390/ijms24076261.
[15] S.Q. Tsai, Z. Zheng, N.T. Nguyen, M. Liebers, V.V. Topkar, V. Thapar, N. Wyvekens, C. Khayter, A.J. Iafrate, L.P. Le, M.J. Aryee, J.K. Joung, GUIDE-seq enables genome-wide profiling of off-target cleavage by CRISPR-Cas nucleases, Nat. Biotechnol. 33 (2015) 187–197, https://doi.org/10.1038/nbt.3117.
[16] B. Wienert, S.K. Wyman, C.D. Richardson, C.D. Yeh, P. Akcakaya, M.J. Porritt, M. Morlock, J.T. Vu, K.R. Kazane, H.L. Watry, L.M. Judge, B.R. Conklin, M. Maresca, J.E. Corn, Unbiased detection of CRISPR off-targets in vivo using DISCOVER-Seq, Science 364 (2019) 286–289, https://doi.org/10.1126/science.aav9023.
[17] S. Bae, J. Park, J.-S. Kim, Cas-OFFinder: a fast and versatile algorithm that searches for potential off-target sites of Cas9 RNA-guided endonucleases, Bioinformatics 30 (2014) 1473–1475, https://doi.org/10.1093/bioinformatics/btu048.
[18] J.-P. Concordet, M. Haeussler, CRISPOR: intuitive guide selection for CRISPR/Cas9 genome editing experiments and screens, Nucleic Acids Res. 46 (2018) W242–W245, https://doi.org/10.1093/nar/gky354.
[19] K. Labun, T.G. Montague, J.A. Gagnon, S.B. Thyme, E. Valen, CHOPCHOP v2: a web tool for the next generation of CRISPR genome engineering, Nucleic Acids Res. 44 (2016) W272–W276, https://doi.org/10.1093/nar/gkw398.
[20] S.Q. Tsai, N.T. Nguyen, J. Malagon-Lopez, V.V. Topkar, M.J. Aryee, J.K. Joung, CIRCLE-seq: a highly sensitive in vitro screen for genome-wide CRISPR-Cas9 nuclease off-targets, Nat. Methods 14 (2017) 607–614, https://doi.org/10.1038/nmeth.4278.
[21] D. Kim, S. Bae, J. Park, E. Kim, S. Kim, H.R. Yu, J. Hwang, J.-I. Kim, J.-S. Kim, Digenome-seq: genome-wide profiling of CRISPR-Cas9 off-target effects in human cells, Nat. Methods 12 (2015) 237-43, 1 p following 243. https://doi.org/10.1038/nmeth.3284.
[22] P. Cameron, C.K. Fuller, P.D. Donohoue, B.N. Jones, M.S. Thompson, M.M. Carter, S. Gradia, B. Vidal, E. Garner, E.M. Slorach, E. Lau, L.M. Banh, A.M. Lied, L. S. Edwards, A.H. Settle, D. Capurso, V. Llaca, S. Deschamps, M. Cigan, J.K. Young, A.P. May, Mapping the genomic landscape of CRISPR-Cas9 cleavage, Nat. Methods 14 (2017) 600–606, https://doi.org/10.1038/nmeth.4284.
[23] J. Hu, R.M. Meyers, J. Dong, R.A. Panchakshari, F.W. Alt, R.L. Frock, Detecting DNA double-stranded breaks in mammalian genomes by linear amplification-mediated high-throughput genome-wide translocation sequencing, Nat. Protoc. 11 (2016) 853–871, https://doi.org/10.1038/nprot.2016.043.
[24] T. Wimmer, B. Lorenz, K. Stieger, Quantification of the vascular endothelial growth factor with a bioluminescence resonance energy transfer (BRET) based single molecule biosensor, Biosens. Bioelectron. 86 (2016) 609–615, https://doi.org/10.1016/j.bios.2016.07.058.
[25] J. Columbus, T. Turbyville, Studying RAS Interactions in Live Cells with BRET, Methods Mol. Biol. 2797 (2024) 253–260, https://doi.org/10.1007/978-1-0716-3822-4_18.
[26] A. Dragulescu-Andrasi, C.T. Chan, A. De, T.F. Massoud, S.S. Gambhir, Bioluminescence resonance energy transfer (BRET) imaging of protein-protein interactions within deep tissues of living subjects, PNAS 108 (2011) 12060–12065, https://doi.org/10.1073/pnas.1100923108.
[27] N.C.H. Le, M. Gel, Y. Zhu, H. Dacres, A. Anderson, S.C. Trowell, Real-time, continuous detection of maltose using bioluminescence resonance energy transfer (BRET) on a microfluidic system, Biosens. Bioelectron. 62 (2014) 177–181, https://doi.org/10.1016/j.bios.2014.06.032.
[28] C. Stumpf, T. Wimmer, B. Lorenz, K. Stieger, Creation of different bioluminescence resonance energy transfer based biosensors with high affinity to VEGF, PLoS One 15 (2020) e0230344, https://doi.org/10.1371/journal.pone.0230344.
[29] T. Wimmer, E. Schroeter, B. Lorenz, K. Stieger, Detection of the Vascular Endothelial Growth Factor with a Novel Bioluminescence Resonance Energy Transfer Pair Using a Two-Component System, Sensors (Basel) 17 (2017), https://doi.org/10.3390/s17010145.
[30] I. Kufareva, B. Stephens, C.T. Gilliland, B. Wu, G. Fenalti, D. Hamel, R.C. Stevens, R. Abagyan, T.M. Handel, A novel approach to quantify G-protein-coupled receptor dimerization equilibrium using bioluminescence resonance energy transfer, Methods Mol. Biol. 1013 (2013) 93–127, https://doi.org/10.1007/978-1-62703-426-5_7.
[31] D. Morse, B.A. Tannous, A water-soluble coelenterazine for sensitive in vivo imaging of coelenterate luciferases, Mol. Ther. 20 (2012) 692–693, https://doi.org/10.1038/mt.2012.38.
[32] H.J. van der Veer, E.A. van Aalen, C.M.S. Michielsen, E.T.L. Hanckmann, J. Deckers, M.M.G.J. van Borren, J. Flipse, A.J.M. Loonen, J.P.H. Schoeber, M. Merkx, Glow-in-the-Dark Infectious Disease Diagnostics Using CRISPR-Cas9-Based Split Luciferase Complementation, ACS Cent. Sci. 9 (2023) 657–667, https://doi.org/10.1021/acscentsci.2c01467.
[33] C.W. White, H.K. Vanyai, H.B. See, E.K.M. Johnstone, K.D.G. Pfleger, Using nanoBRET and CRISPR/Cas9 to monitor proximity to a genome-edited protein in real-time, Sci. Rep. 7 (2017) 3187, https://doi.org/10.1038/s41598-017-03486-2.
[34] T. Wimmer, D. Bonthu, V. Moeschl, P. Kleekamp, C. Thiel, L. Lytvynchuk, M. Ellinwood, K. Stieger, A Bioluminescence Resonance Energy Transfer-Based Reporter System: Characterization and Applications, CRISPR J. 4 (2021) 884–895, https://doi.org/10.1089/crispr.2021.0023.
[35] J. Icha, M. Weber, J.C. Waters, C. Norden, Phototoxicity in live fluorescence microscopy, and how to avoid it, Bioessays 39 (2017), https://doi.org/10.1002/bies.201700003.
[36] F.A. Ran, P.D. Hsu, J. Wright, V. Agarwala, D.A. Scott, F. Zhang, Genome engineering using the CRISPR-Cas9 system, Nat. Protoc. 8 (2013) 2281–2308, https://doi.org/10.1038/nprot.2013.143.
[37] S. Sun, X. Yang, Y. Wang, X. Shen, In Vivo Analysis of Protein-Protein Interactions with Bioluminescence Resonance Energy Transfer (BRET): Progress and Prospects, Int. J. Mol. Sci. 17 (2016), https://doi.org/10.3390/ijms17101704.
[38] A.P. May, P. Cameron, A.H. Settle, C.K. Fuller, M.S. Thompson, A.M. Cigan, J.K. Young, SITE-Seq: A Genome-wide Method to Measure Cas9 Cleavage (2023). https://doi.org/10.21203/rs.3.nprot-5889/v2.
[39] C. Guo, X. Ma, F. Gao, Y. Guo, Off-target effects in CRISPR/Cas9 gene editing, Front. Bioeng. Biotechnol. 11 (2023) 1143157, https://doi.org/10.3389/fbioe.2023.1143157.
[40] Y. Fu, J.D. Sander, D. Reyon, V.M. Cascio, J.K. Joung, Improving CRISPR-Cas nuclease specificity using truncated guide RNAs, Nat. Biotechnol. 32 (2014) 279–284, https://doi.org/10.1038/nbt.2808.
[41] D.E. Ryan, D. Taussig, I. Steinfeld, S.M. Phadnis, B.D. Lunstad, M. Singh, X. Vuong, K.D. Okochi, R. McCaffrey, M. Olesiak, S. Roy, C.W. Yung, B. Curry, J.R. Sampson, L. Bruhn, D.J. Dellinger, Improving CRISPR-Cas specificity with chemical modifications in single-guide RNAs, Nucleic Acids Res. 46 (2018) 792–803, https://doi.org/10.1093/nar/gkx1199.
[42] Y. Lin, T.J. Cradick, M.T. Brown, H. Deshmukh, P. Ranjan, N. Sarode, B.M. Wile, P. M. Vertino, F.J. Stewart, G. Bao, CRISPR/Cas9 systems have off-target activity with insertions or deletions between target DNA and guide RNA sequences, Nucleic Acids Res. 42 (2014) 7473–7485, https://doi.org/10.1093/nar/gku402.
[43] G.I. Corsi, K. Qu, F. Alkan, X. Pan, Y. Luo, J. Gorodkin, CRISPR/Cas9 gRNA activity depends on free energy changes and on the target PAM context, Nat. Commun. 13 (2022) 3006, https://doi.org/10.1038/s41467-022-30515-0.
[44] E.A. Boyle, W.R. Becker, H.B. Bai, J.S. Chen, J.A. Doudna, W.J. Greenleaf, Quantification of Cas9 binding and cleavage across diverse guide sequences maps landscapes of target engagement, Sci. Adv. 7 (2021), https://doi.org/10.1126/sciadv.abe5496.
[45] C. Kuscu, S. Arslan, R. Singh, J. Thorpe, M. Adli, Genome-wide analysis reveals characteristics of off-target sites bound by the Cas9 endonuclease, Nat. Biotechnol. 32 (2014) 677–683, https://doi.org/10.1038/nbt.2916.
[46] J.P.K. Bravo, M.-S. Liu, G.N. Hibshman, T.L. Dangerfield, K. Jung, R.S. McCool, K. A. Johnson, D.W. Taylor, Structural basis for mismatch surveillance by CRISPR-Cas9, Nature 603 (2022) 343–347, https://doi.org/10.1038/s41586-022-04470-1.
[47] M. Pacesa, C.-H. Lin, A. Cléry, A. Saha, P.R. Arantes, K. Bargsten, M.J. Irby, F.-H.-T. Allain, G. Palermo, P. Cameron, P.D. Donohoue, M. Jinek, Structural basis for Cas9 off-target activity, Cell 185 (2022) 4067–4081.e21, https://doi.org/10.1016/j.cell.2022.09.026.
[48] X. Chen, M.A.F.V. Gonçalves, DNA, RNA, and Protein Tools for Editing the Genetic Information in Human Cells, iScience 6 (2018) 247–263. https://doi.org/10.1016/j.isci.2018.08.001.